

# Infrared and far-infrared laser magnetic resonance spectroscopy of the GeH radical: Determination of ground state parameters<sup>a)</sup>

John M. Brown<sup>b)</sup>

*Department of Chemistry, University of Southampton, Southampton SO9 5NH, England*

K. M. Evenson

*National Bureau of Standards, Boulder, Colorado 80303*

Trevor J. Sears

*Chemistry Department, Brookhaven National Laboratory, Upton, New York 11973*

(Received 22 May 1985; accepted 18 June 1985)

The GeH radical has been detected in its ground  $^2\Pi$  state in the gas phase reaction of fluorine atoms with GeH<sub>4</sub> by laser magnetic resonance techniques. Rotational transitions within both  $^2\Pi_{1/2}$  and  $^2\Pi_{3/2}$  manifolds have been observed at far-infrared wavelengths and rotational transitions between the two fine structure components have been detected at infrared wavelengths (10  $\mu\text{m}$ ). Signals have been observed for all five naturally occurring isotopes of germanium. Nuclear hyperfine structure for  $^1\text{H}$  and  $^{73}\text{Ge}$  has also been observed. The data for the dominant isotope ( $^{74}\text{GeH}$ ) have been fitted to within experimental error by an effective Hamiltonian to give a set of molecular parameters for the  $X^2\Pi$  state which is very nearly complete. In addition, the dipole moment of GeH in its ground state has been estimated from the relative intensities of electric and magnetic dipole transitions in the 10  $\mu\text{m}$  spectrum to be  $1.24(\pm 0.10)$  D.

## I. INTRODUCTION

The GeH radical was first detected by Kleman and Werhagen<sup>1,2</sup> who observed two electronic band systems, in the visible and near-ultraviolet regions of the spectrum. Analysis of the rotational structure confirmed the assignment of the spectra to the  $a^4\Sigma^- - X^2\Pi$  and  $A^2\Delta - X^2\Pi$  transitions, respectively. Shortly afterwards, Barrow, Drummond, and Garton<sup>3</sup> reported another band system in the ultraviolet which is probably the  $B^2\Sigma^- - X^2\Pi$  transition although a detailed analysis has not yet been performed. The spectra were complicated somewhat by the fact that germanium has five naturally occurring isotopes, although only three of these have abundances greater than 10% ( $^{74}\text{Ge}$  36.7%,  $^{72}\text{Ge}$  27.4%, and  $^{70}\text{Ge}$  20.6%). The isotopic structure broadens the lines in the optical spectra but is not fully resolved. This was the case even in the higher resolution study of the  $A^2\Delta - X^2\Pi$  system by Klynning and Lindgren,<sup>4</sup> who fitted their measurements and obtained values for the major molecular parameters for both the states involved. More recently, Veseeth<sup>5</sup> reanalyzed the same data in terms of a different Hamiltonian and presented an alternative set of molecular parameters. However these seem to be the only spectroscopic observations of GeH before the present work.

In common with all the group IV diatomic hydrides, the ground state of GeH is a regular  $^2\Pi$  state. However the involvement of the heavy atom causes the spin-orbit interaction to be large and results in a big separation between the  $^2\Pi_{3/2}$  and  $^2\Pi_{1/2}$  fine structure components. This splitting is about 900  $\text{cm}^{-1}$  for GeH so that the proportion of molecules in levels of the upper,  $^2\Pi_{3/2}$  component is rather small at ambient temperatures. Since GeH in levels of the  $^2\Pi_{1/2}$  component is only weakly magnetic, its EPR spectrum has not

yet been detected. Indeed, until the present work, there has been no experimental information on the molecule's  $g$  factors or nuclear hyperfine structure. In this paper, we report the observation of rotational transitions between levels in each of the fine structure components of GeH by the technique of far-infrared laser magnetic resonance (LMR)<sup>6</sup> and also the detection of weak, magnetic-dipole transitions between the  $\Omega = 3/2$  and  $\Omega = 1/2$  levels by infrared LMR<sup>7</sup> using a CO<sub>2</sub> laser as the radiation source. The molecule was generated by the reaction between F atoms and germane (GeH<sub>4</sub>), a method suggested by earlier work on the analogous molecule CH.<sup>8,9</sup> The corresponding reaction was also used to observe the SiH radical.<sup>10</sup> The resolution of the magnetic resonance experiments was easily high enough to permit transitions for the different germanium isotopes to be resolved. Far from being a hindrance, the isotopic structure was a powerful aid in the assignment of the spectra. The far-infrared LMR signals were impressively strong, particularly so when it is realized that neither fine structure component is favorable for detection by magnetic resonance techniques (the  $^2\Pi_{1/2}$  component because of poor tunability and the  $^2\Pi_{3/2}$  component because of low relative population).

The analysis of the observed spectra leads to a complete and very precise determination of the molecular parameters for GeH in its ground  $^2\Pi$  state. For the  $^2\Pi_{1/2}$  transitions, splittings due to the  $^1\text{H}$  hyperfine interaction were observed. Of the germanium isotopes, only  $^{73}\text{Ge}$  with  $I = 9/2$  has a nonzero spin. It was present in natural abundance of 7.7% and we were able to detect signals which showed hyperfine structure from  $^{73}\text{GeH}$  for the higher frequency transitions in the  $^2\Pi_{3/2}$  component. Both  $^1\text{H}$  and  $^{73}\text{Ge}$  hyperfine splittings provide information about the electronic wave functions for the  $X^2\Pi$  state. In addition, four of the six primary molecular  $g$  factors were well determined by the data and also provide information on the electronic structure of GeH. In addition, we have been able to make an estimate of the electric dipole

<sup>a)</sup> Work supported in part by NASA contract W-15, 047.

<sup>b)</sup> Present address: Physical Chemistry Laboratory, South Parks Road, Oxford, OX1 3QZ, England.

TABLE I. Summary of transitions observed in GeH in the  $v = 0$  level of the  $X^2\Pi$  state by LMR.

Transition		Laser line		
Spin component	$J' \leftarrow J''$	$\lambda / \mu\text{m}$	$\nu / \text{MHz}$	Lasing gas
$^2\Pi_{1/2}$	$3/2^- \leftarrow 1/2^{+a}$	513.0	584 387.7 <sup>b</sup>	HCOOH
	$3/2^+ \leftarrow 1/2^-$	500.6	598 893.7 <sup>c</sup>	CD <sub>2</sub> F <sub>2</sub>
	$5/2^- \leftarrow 3/2^+$	302.0	992 708.9 <sup>d</sup>	CH <sub>3</sub> OH
$^2\Pi_{3/2}$	$5/2^\pm \leftarrow 3/2^\mp$	302.0	992 708.9 <sup>d</sup>	CH <sub>3</sub> OH
	$7/2^\pm \leftarrow 5/2^\mp$	215.4	1 391 972.1 <sup>e</sup>	CH <sub>3</sub> OD
		214.6	1 397 118.6 <sup>f</sup>	CH <sub>2</sub> F <sub>2</sub>
		166.6	1 799 139.3 <sup>f</sup>	CH <sub>2</sub> F <sub>2</sub>
$^2\Pi_{3/2} \leftarrow ^2\Pi_{1/2}$	$3/2^\pm \leftarrow 3/2^-$	11.359	26 392 844 <sup>g</sup>	<sup>13</sup> CO <sub>2</sub>
	$3/2^- \leftarrow 1/2^-$	11.128	26 940 814 <sup>g</sup>	<sup>13</sup> CO <sub>2</sub>
	$5/2^- \leftarrow 3/2^-$	10.945	27 390 373 <sup>g</sup>	<sup>13</sup> C <sup>18</sup> O <sub>2</sub>

<sup>a</sup>Superscripts refer to the parities of the levels involved.

<sup>b</sup>H. E. Radford, F. R. Petersen, D. A. Jennings, and J. A. Mucha, IEEE J. Quantum Electron. QE-13, 92 (1977).

<sup>c</sup>E. C. C. Vasconcellos, F. R. Petersen, and K. M. Evenson, Int. J. IR Mm Waves 2, 705 (1981).

<sup>d</sup>F. R. Petersen, K. M. Evenson, D. A. Jennings, and A. Scalabrin, IEEE J. Quantum Electron. QE-16, 319 (1980).

<sup>e</sup>T. G. Blaney, D. J. E. Knight, and E. K. Murray-Lloyd, Opt. Commun. 25, 176 (1978).

<sup>f</sup>F. R. Petersen, A. Scalabrin, and K. M. Evenson, Int. J. IR Mm Waves 1, 111 (1980).

<sup>g</sup>C. Freed, L. C. Bradley, and R. G. O'Donnell, IEEE J. Quantum Electron. QE-16, 1195 (1980).

moment of GeH by a comparison of the intensities of electric and magnetic dipole transitions in the 10  $\mu\text{m}$  spectra. The value obtained is "normal," not anomalously small as in the case of SiH.<sup>10</sup>

## II. EXPERIMENTAL DETAILS AND RESULTS

The far-infrared LMR spectra were recorded at the Boulder Laboratories of the National Bureau of Standards using the FIR LMR spectrometer described previously.<sup>6</sup> GeH radicals were generated in the gas phase in a continuous flow reaction between fluorine atoms, generated by a microwave discharge in a mixture of fluorine and helium, and germane, GeH<sub>4</sub>, which was obtained commercially. The reaction occurred in the sample region of the far-infrared laser cavity which was located between the pole pieces of a 38 cm electromagnet. The total pressure used was about 52 Pa (400 mTorr) with partial pressures of F<sub>2</sub>/F and GeH<sub>4</sub> approximately equal at 9 Pa (70 mTorr). The strongest GeH signals were observed when the partial pressure of GeH<sub>4</sub> was slightly more than that required to maximize the violet chemiluminescence produced in the reaction. Magnetic flux densities were measured by a rotating coil probe which was calibrated periodically against a proton NMR gaussmeter. The overall uncertainty in flux measurements is:  $10^{-5}$  T below 0.1 T and  $10^{-4} \times B_0$  above 0.1 T where  $B_0$  is the magnetic flux density. The far-infrared laser frequencies used in this work are given in Table I. The uncertainties in these arise mainly from irreproducibility in setting the laser to the peak of the gain profile (see references given). We believe that this uncertainty ( $1\sigma$ ) is not more than 2 MHz for the laser lines employed.

The observed LMR spectra of the GeH radical in the  $v = 0$  level of the  $X^2\Pi$  state at far- and mid-infrared wavelengths are summarized in Table I. The rotational transitions involved are also shown in the energy level diagram of

Fig. 1. In the far-infrared spectrum, measurements were made on the Zeeman components of three different transitions in the  $^2\Pi_{1/2}$  manifold and of six different transitions in

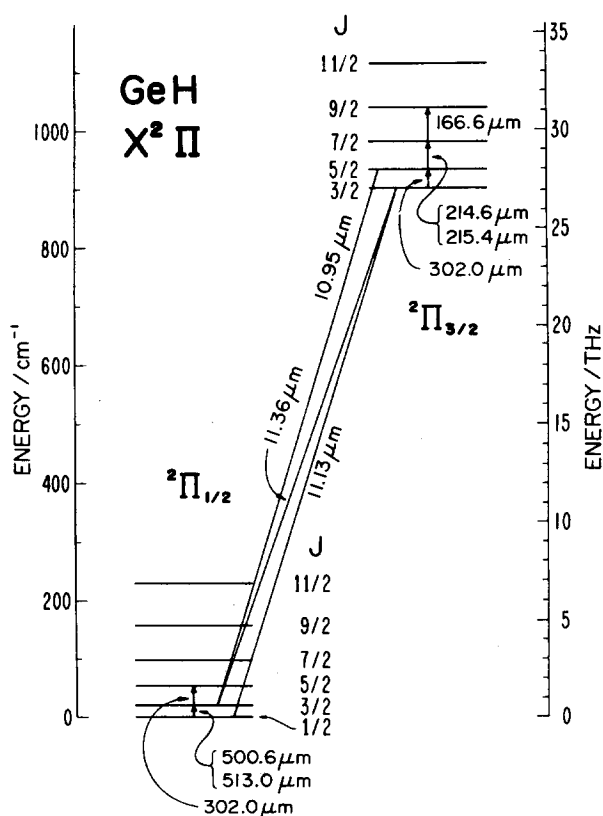


FIG. 1. Diagram showing the lower energy levels of GeH in the  $X^2\Pi$  state and the transitions involved in the present work. The rotational transitions were studied in a far-IR LMR spectrometer whereas the fine structure transitions were studied in the mid-IR. Note that the levels of the upper,  $^2\Pi_{3/2}$  component are considerably higher in energy than those of the  $^2\Pi_{1/2}$  component.

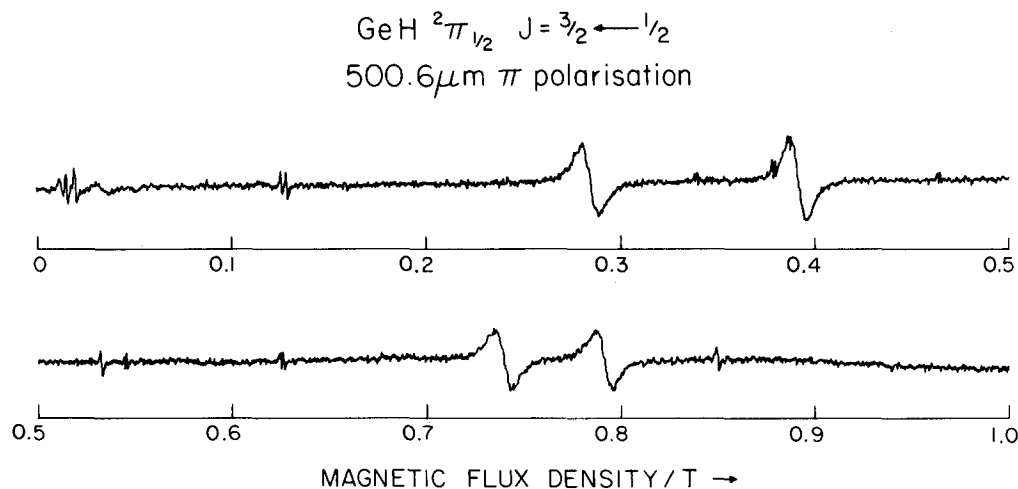


FIG. 2. Part of the 500.6  $\mu\text{m}$  LMR spectrum of GeH, recorded with the oscillating electric field parallel to the applied magnetic field ( $\pi$  polarization). The rotational transition involved is  $J = 1\frac{1}{2} \leftarrow \frac{1}{2}$  in the  ${}^2\Pi_{1/2}$  component. The broad lines belong to GeH, the lower field doublet involving  ${}^{74}\text{GeH}$  and the upper  ${}^{72}\text{GeH}$ . The doublet splitting arises from the proton hyperfine interaction and has a different magnitude for the two isotopes because different  $M_J$  components are involved in the two transitions. The GeH lines are broad because the transitions involved in the  ${}^2\Pi_{1/2}$  component tune very slowly with applied magnetic field. The weaker, sharper lines arise from unidentified impurities.

the  ${}^2\Pi_{3/2}$  manifold. Examples of the spectra are shown in Figs. 2 and 3. Figure 2 shows part of the spectrum recorded with the 500.6  $\mu\text{m}$   $\text{CH}_2\text{F}_2$  laser line with the electric vector of the far IR radiation parallel with the applied magnetic field ( $\pi$  polarization). The strong, broad lines are components of the  $J = 3/2 \leftarrow 1/2$ ,  $+ \leftarrow -$  rotational transition in the  ${}^2\Pi_{1/2}$  manifold of both  ${}^{74}\text{GeH}$  (at 0.28 and 0.39 T) and  ${}^{72}\text{GeH}$  (at 0.74 and 0.79 T). The doublet structure for each isotopic species arises from the proton hyperfine interaction (the splittings are different in magnitude because different  $M_J$  components are involved, see below). Two aspects of the  ${}^2\Pi_{1/2}$  transitions should be appreciated. First, it is rather remarkable that such transitions are seen at all. Unlike other examples of so-called  ${}^2\Pi_{1/2}$  transitions in lighter molecules (e.g.,  $\text{CH}^9$  and  $\text{SiH}^{10}$ ), the levels of the  ${}^2\Pi_{1/2}$  component in

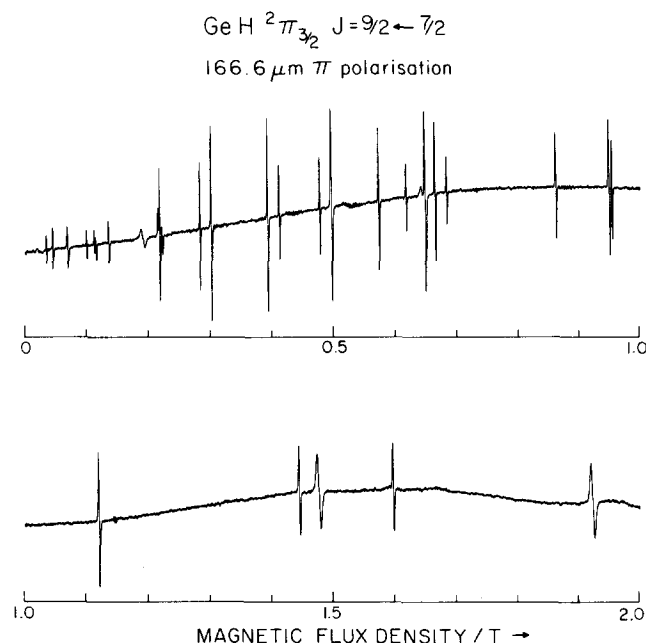


FIG. 3. The 166.6  $\mu\text{m}$  LMR spectrum of GeH, recorded with the oscillating electric field parallel to the applied magnetic field. The rotational transition involved is  $J = 4\frac{1}{2} \leftarrow 3\frac{1}{2}$  in the  ${}^2\Pi_{3/2}$  spin component. Lines from all five naturally occurring isotopes of germanium are observed which makes the spectrum appear more complicated. The weak ten-line hyperfine patterns of  ${}^{73}\text{GeH}$  ( $I = 4\frac{1}{2}$ ) are just discernible in the first half of the spectrum between 0.3 and 1.0 T. It is also just possible to make out Lamb dips on some of the stronger, broader lines.

GeH are essentially uncontaminated by those of the  ${}^2\Pi_{3/2}$  component and the magnetic moments associated with these levels are indeed very small. The transitions therefore tune very slowly ( $\sim 0.02$  MHz/G) and their observation by LMR requires the happy accident of a very close coincidence between molecular and laser frequencies. Consequently, the observed resonances are very broad. The second point to be appreciated is that the lines are also very strong since the integrated intensity of the signals is proportional to the square of the linewidth. In our experiments they were also severely under modulated; our maximum modulation amplitude at 12 kHz was about 1 mT (10 G). By contrast, Fig. 3 shows a more familiar type of LMR spectrum involving a transition in the  ${}^2\Pi_{3/2}$  manifold. It depicts a broad scan taken with the laser oscillating on the 166.6  $\mu\text{m}$  line of  $\text{CH}_2\text{F}_2$  in parallel ( $\pi$ ) polarization. The resonances are associated with both lambda doublets of the  $J = 9/2 \leftarrow 7/2$  transition of GeH in the  ${}^2\Pi_{3/2}$  state. The spectrum is complicated, at least superficially, by manifestations of all five naturally occurring isotopes of germanium. Although no special effort was made to record Lamb (saturation) dips on these signals, all the strongest lines in the 166.6  $\mu\text{m}$  spectrum showed them. The observed resonances in the far IR LMR spectra of all the naturally occurring isotopes of GeH except  ${}^{73}\text{Ge}$  are given in Table II.  ${}^{73}\text{Ge}$  has a natural abundance of 7.7% and a spin of 9/2. The intensity of each of its transitions is therefore divided among ten hyperfine components (if the proton hfs is not resolved) and its resonances are consequently much weaker than those of the other isotopes. Lines for  ${}^{73}\text{GeH}$  were nevertheless detected in the 214.6 and 166.6  $\mu\text{m}$  spectra and are just discernible in Fig. 3. The hyperfine splittings of the  ${}^{73}\text{GeH}$  lines contain information about the hyperfine parameters; some measurements of the strongest features are given in Table IV.

Although the far IR data may be used to characterize the energy level structure within each fine structure component very precisely, they are rather insensitive to the value for the spin-orbit coupling constant  $A$  which determines the separation between the two components. For molecules with large spin-orbit splitting, such as GeH, this quantity has been difficult to measure accurately because direct electric dipole transitions between the two components are forbidden in the limit of Hund's case (a) coupling.<sup>11</sup> Recently how-

TABLE II. Measurements of the observed resonances in (in mT) in the LMR spectra of GeH and fit of the data for  $^{74}\text{GeH}$ .

$M_J$	$M_I$	Parity	$^{70}\text{GeH}$	$^{72}\text{GeH}$	$^{74}\text{GeH}$	$^{76}\text{GeH}$	(obs-calc) for $^{74}\text{GeH}/\text{MHz}$	
$513.0 \mu\text{m } \nu_L = 584\,387.7 \text{ MHz } ^2\Pi_{1/2}, J = 3/2 \leftarrow 1/2 (- \leftarrow +)$								
$\sigma$	$1/2 \leftarrow - 1/2$	$1/2 \leftarrow 1/2$	$- \leftarrow +$	213.5	861.3	1471.9	a	-0.65
		$- 1/2 \leftarrow - 1/2$		238.0	883.0	1493.2	a	-0.63
	$3/2 \leftarrow 1/2$	$- 1/2 \leftarrow - 1/2$	$- \leftarrow +$	241.5	963.0	1649.4	a	1.18
		$1/2 \leftarrow 1/2$		260.5	982.5	1669.9	a	0.68
$500.6 \mu\text{m } \nu_L = 598\,893.7 \text{ MHz } ^2\Pi_{1/2}, J = 3/2 \leftarrow 1/2 (+ \leftarrow -)$								
$\pi$	$1/2 \leftarrow 1/2$	$- 1/2 \leftarrow - 1/2$	$+ \leftarrow -$	a	a	286.3	1357.5	0.77
		$1/2 \leftarrow 1/2$		a	a	393.6	1432.5	1.09
	$- 1/2 \leftarrow - 1/2$	$- 1/2 \leftarrow - 1/2$	$+ \leftarrow -$	1938.0	740.0	a	a	
		$1/2 \leftarrow 1/2$		a	793.0	a	a	
$\sigma$	$3/2 \leftarrow 1/2$	$- 1/2 \leftarrow - 1/2$	$+ \leftarrow -$	a	a	243.0	1124.2	0.68
		$1/2 \leftarrow 1/2$		a	a	290.8	1146.7	0.60
	$- 1/2 \leftarrow 1/2$	$- 1/2 \leftarrow - 1/2$	$+ \leftarrow -$	a	a	367.0	b	0.39
		$1/2 \leftarrow 1/2$		a	a	547.0	b	1.46
	$- 1/2 \leftarrow - 3/2$	$- 1/2 \leftarrow - 1/2$	$+ \leftarrow -$	1540.7	605.6	a	a	
		$1/2 \leftarrow 1/2$		1553.8	609.6	a	a	
	$1/2 \leftarrow - 1/2$	$- 1/2 \leftarrow - 1/2$	$+ \leftarrow -$	a	957.7	a	a	
		$1/2 \leftarrow 1/2$		a	1090.1	a	a	
$302.0 \mu\text{m } \nu_L = 992\,708.9 \text{ MHz } ^2\Pi_{1/2}, J = 5/2 \leftarrow 3/2 (- \leftarrow +)$								
$\pi$	$3/2 \leftarrow 3/2$	$- 1/2 \leftarrow - 1/2$	$- \leftarrow +$	a	a	657.1	a	-0.23
		$1/2 \leftarrow 1/2$		a	a	708.1	a	-0.25
$\sigma$	$5/2 \leftarrow 1/2$	$- 1/2 \leftarrow 1/2$	$- \leftarrow +$	a	a	250.5	b	-0.55
	$5/2 \leftarrow 3/2$	$1/2 \leftarrow 1/2$		a	a	332.8	1777.5	-0.80
		$- 1/2 \leftarrow - 1/2$		a	a	332.8	1777.5	-0.41
	$3/2 \leftarrow 1/2$	$1/2 \leftarrow 1/2$	$- \leftarrow +$	a	a	468.4	a	-0.93
		$- 1/2 \leftarrow - 1/2$		a	a	497.2	a	-0.38
	$1/2 \leftarrow - 1/2$	$1/2 \leftarrow 1/2$	$- \leftarrow +$	a	a	860.0	a	-0.93
		$- 1/2 \leftarrow - 1/2$		a	a	947.5	a	-0.57
	$- 5/2 \leftarrow - 3/2$	$1/2 \leftarrow 1/2$	$- \leftarrow +$	a	1184.0	a	a	
		$- 1/2 \leftarrow - 1/2$		a	1190.8	a	a	
	$- 3/2 \leftarrow - 1/2$	$1/2 \leftarrow 1/2$	$- \leftarrow +$	a	1724.4	a	a	
		$- 1/2 \leftarrow - 1/2$		a	1734.0	a	a	
$302.0 \mu\text{m } \nu_L = 992\,708.9 \text{ MHz } ^2\Pi_{3/2}, J = 5/2 \leftarrow 3/2$								
$\pi$	$3/2 \leftarrow 3/2$		$+ \leftarrow -$	990.5	949.1	909.6	c	-2.91
			$- \leftarrow +$	997.7	956.2	916.7	879.5	-3.25
$\sigma$	$- 1/2 \leftarrow 1/2$		$+ \leftarrow -$	1236.4	1183.8	1134.2	b	0.08
			$- \leftarrow +$	1245.8	1193.2	1143.5	b	-0.05
	$5/2 \leftarrow 3/2$		$+ \leftarrow -$	1909.1	1829.1	1752.9	1680.6	-0.44
			$- \leftarrow +$	1922.8	1842.2	1766.0	1693.6	-0.35
$215.4 \mu\text{m } \nu_L = 1\,391\,972.1 \text{ MHz } ^2\Pi_{3/2}, J = 7/2 \leftarrow 5/2$								
$\sigma$	$3/2 \leftarrow 5/2$		$- \leftarrow +$	1315.2	1243.2	1175.0	(1110.6)	-1.69
			$+ \leftarrow -$	1333.3	1261.1	1192.8	(1128.5)	-2.53
$214.6 \mu\text{m } \nu_L = 1\,397\,118.6 \text{ MHz } ^2\Pi_{3/2}, J = 7/2 \leftarrow 5/2$								
$\pi$	$5/2 \leftarrow 5/2$		$- \leftarrow +$	949.4	844.6	745.6	652.0	1.29
			$+ \leftarrow -$	975.0	870.3	771.3	677.6	1.32
	$3/2 \leftarrow 3/2$		$- \leftarrow +$	1583.7	1409.1	1244.0	1087.7	2.23
			$+ \leftarrow -$	1626.9	1452.0	1286.7	1130.5	1.73
$\sigma$	$3/2 \leftarrow 5/2$		$- \leftarrow +$	646.8	575.6	508.2	b	-0.95
			$+ \leftarrow -$	664.5	593.2	526.0	b	0.00
	$1/2 \leftarrow 3/2$		$- \leftarrow +$	889.2	791.5	699.2	611.5	0.59

TABLE II (continued).

$M_J$	$M_I$	Parity	$^{70}\text{GeH}$	$^{72}\text{GeH}$	$^{74}\text{GeH}$	$^{76}\text{GeH}$	(obs-calc) for $^{74}\text{GeH}/\text{MHz}$
		+ ← -	914.0	816.0	723.5	635.8	0.08
- 1/2 ←	1/2	- ← +	1423.4	1266.9	1119.4	979.1	1.38
		+ ← -	1439.0	1306.3	1158.5	1018.3	0.63
7/2 ←	5/2	- ← +	1774.3	1577.6	1392.0	1216.8	0.47
		+ ← -	1821.1	1624.4	1439.0	1263.5	1.33
$166.6 \mu\text{m } \nu_L = 1\,799\,139.3 \text{ MHz } ^2\Pi_{3/2}, J = 9/2 \leftarrow 7/2$							
$\pi$							
7/2 ←	7/2	+ ← -	620.9	411.1	213.3	26.2	0.06
		- ← +	688.5	477.8	279.8	92.8	-0.76
5/2 ←	5/2	+ ← -	869.8	575.2	298.5	36.7	-0.05
		- ← +	962.2	669.5	391.7	130.5	-0.50
3/2 ←	3/2	+ ← -	1444.9	957.1	497.2	61.8	0.15
		- ← +	1600.5	1113.5	653.2	216.7	1.16
1/2 ←	1/2	+ ← -	a	a	1477.4	186.9	1.04
		- ← +	a	a	1932.0	648.0	1.36
$\sigma$							
5/2 ←	7/2	+ ← -	429.8	285.0	148.0	b	0.88
		- ← +	c	331.2	c	b	
3/2 ←	5/2	+ ← -	535.7	354.9	184.5	22.5	1.97
		- ← +	594.2	412.7	241.9	80.2	-0.93
1/2 ←	3/2	+ ← -	710.3	417.0	244.5	30.0	-0.49
		- ← +	788.1	548.2	321.2	106.8	-0.89
- 1/2 ←	1/2	+ ← -	1054.4	700.4	363.5	44.9	-0.56
		- ← +	1169.4	814.1	478.0	c	-0.30
9/2 ←	7/2	+ ← -	1114.6	737.7	382.2	46.9	-0.39
		- ← +	1233.0	856.2	501.0	165.6	-0.64
- 3/2 ←	- 1/2	+ ← -	a	1356.5	707.5	87.5	-0.54
		- ← +	a	1579.6	930.6	309.5	-0.35
7/2 ←	5/2	+ ← -	a	1505.5	782.2	96.3	-0.02
		- ← +	a	1742.7	1021.8	338.9	-0.58
$11.36 \mu\text{m } \nu_L = 26\,392\,844 \text{ MHz } ^2\Pi_{3/2} \leftarrow ^2\Pi_{1/2}, J = 3/2 \leftarrow 3/2$							
$\pi$							
3/2 ←	1/2	- ← -	c	c	513.3	b	-22.0
3/2 ←	3/2	+ ← -	539.2	531.0	522.3	c	-11.5
$\sigma$							
3/2 ←	1/2	+ ← -	c	c	511.26	b	-11.0
3/2 ←	3/2	- ← -	537.7	529.7	523.3	c	-5.7
$11.13 \mu\text{m } \nu_L = 26\,940\,814 \text{ MHz } ^2\Pi_{3/2} \leftarrow ^2\Pi_{1/2}, J = 3/2 \leftarrow 1/2$							
$\pi$							
- 3/2 ←	- 1/2	- ← -	759.1	753.5	748.6	c	67.0
$10.945 \mu\text{m } \nu_L = 27\,390\,373 \text{ MHz } ^2\Pi_{3/2} \leftarrow ^2\Pi_{1/2}, J = 5/2 \leftarrow 3/2$							
$\pi$							
5/2 ←	3/2	- ← -	d	d	399.7	d	-3.4
3/2 ←	1/2	- ← -	d	d	653.1	d	-13.3

<sup>a</sup>Transitions beyond range of available laboratory field (2 T).

<sup>b</sup>Transition too weak to be observed.

<sup>c</sup>Transition masked by stronger line.

<sup>d</sup>Lines not recorded. Isotopically enriched  $^{74}\text{GeH}_4$  used to record spectrum.

ever, magnetic dipole transitions between the fine structure components of the ground  $^2\Pi$  states of  $\text{SeH}^{12}$  and  $\text{BrO}^{13}$  have been detected by midinfrared LMR. The success of these studies suggested that the corresponding transitions in GeH, for which the fine structure interval lies conveniently in the  $\text{CO}_2$  laser region, should be detectable in the same way.

The infrared LMR measurements were made at the National Research Council in Ottawa using the  $\text{CO}_2$  LMR spectrometer described previously.<sup>7,14,15</sup> The GeH radicals were generated in a similar continuous flow system by the reaction between F atoms and germane. The reactants were mixed in the laser cavity in a region between the pole pieces of a 15 cm electromagnet.  $\text{CF}_4$  was used in the microwave

discharge instead of  $\text{F}_2/\text{He}$  to produce the F atoms because this discharge was quieter, an important feature for the infrared experiment because the discharge was inside the laser cavity. The total pressure used was typically 50 Pa (400 mTorr) and the strongest signals were observed under conditions where the violet chemiluminescence was approximately maximized. The partial pressure of germane was about 2 Pa (15 mTorr).

The  $\text{CO}_2$  laser lines used are given in Table I and the observed resonances in the midinfrared LMR spectrum are given in Table II. Some experiments were performed with isotopically enriched  $^{74}\text{GeH}_4$  to aid identification of the lines and to provide more reliable measurements for the dominant

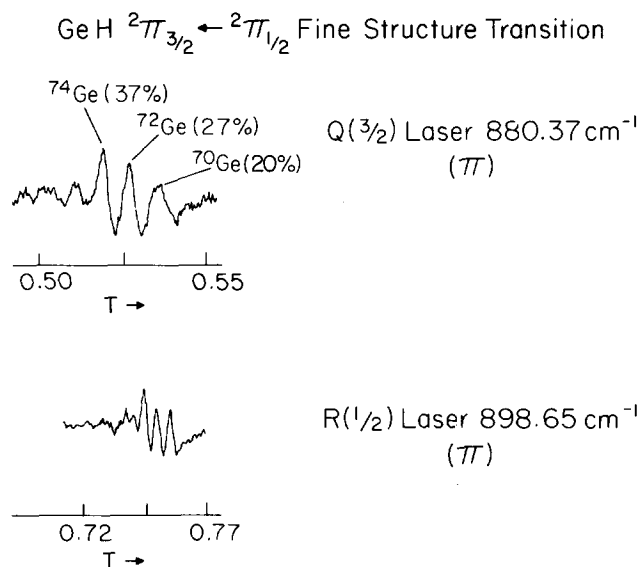


FIG. 4. Two parts of the midinfrared LMR spectrum of the GeH radical, both recorded with the oscillating electric field parallel to the applied magnetic field. The lines can be identified by the presence of the different isotopes of germanium, present in natural abundance. The linewidths are Doppler limited and thus are much broader than those in the far-infrared LMR spectra (see Figs. 2 and 3). The upper spectrum recorded at  $880.37\text{ cm}^{-1}$  shows one of the regions used to determine the electric dipole moment of GeH. The strong  $^{74}\text{GeH}$  line is an electric dipole transition while the weaker line to its left is a magnetic dipole transition for the same isotopic species. The intensities of these two lines were compared in experiments using isotopically enriched  $^{74}\text{GeH}_4$  to minimize distortion by overlap of lines from other isotopes.

isotope. As was the case for SeH<sup>12</sup> and BrO,<sup>13</sup> the strongest transitions were magnetic dipole in character although two resonances in the  $Q(3/2)$  spectrum at  $880.38\text{ cm}^{-1}$  were assigned to particularly strong electric dipole transitions. This permitted an estimate of the electric dipole moment (see below). Components of three separate rotational transitions between the fine structure components were observed. Despite careful searching, no other lines which could be assigned to fine structure transitions were detected. The situation was hampered by the weakness of the spectrum (the strongest lines had a signal-to-noise ratio of less than 10:1 with a 3 s time constant) and by the presence of much stron-

ger resonances which we believe arise from vibration-rotation transitions in the GeH<sub>3</sub> radical. Further work on this spectrum is in progress. Figure 4 shows the LMR spectra of GeH observed with the  $880.38$  and  $898.65\text{ cm}^{-1}$  lines of the  $^{13}\text{C}^{16}\text{O}_2$  laser. The resonances are assigned to the fastest tuning components of the  $Q(3/2)$  and  $R(1/2)$  transitions, respectively. The germanium isotope structure forms a characteristic pattern in these spectra and is of considerable help in the assignment.<sup>12</sup> It is not possible given the available CO<sub>2</sub> laser lines to detect any  $P$ -branch ( $\Delta J = -1$ ) transitions because they occur at too low frequencies.

### III. ANALYSIS

We have chosen to analyze the spectra of GeH in its  $X^2\Pi$  state in terms of an effective Hamiltonian for a diatomic molecule, as described by Brown *et al.*<sup>16-18</sup> The advantages of analyzing spectroscopic data in terms of a soundly based effective Hamiltonian have been discussed previously.<sup>17</sup> The principal one is that it separates the task of data reduction from the interpretation of the molecular parameters. In the present case, a model which made explicit reference to perturbing, excited electronic states would be rather difficult to implement because there are low lying  $^2\Delta$ ,  $^2\Sigma$ , and  $^4\Sigma$  states all of which can contaminate the ground  $^2\Pi$  state. The Hamiltonian used is as follows:

$$H_{\text{eff}} = H_{\text{rot}} + H_{\text{cd}} + H_{\text{so}} + H_{\text{sr}} + H_{\text{LD}} + H_{\text{hfs}} + H_{\text{Z}}, \quad (1)$$

where  $H_{\text{rot}}$  and  $H_{\text{cd}}$  are the rotational and centrifugal distortion terms,  $H_{\text{so}}$  and  $H_{\text{sr}}$  are the spin-orbit and spin-rotation coupling terms,  $H_{\text{LD}}$  is the lambda-doubling contribution,  $H_{\text{hfs}}$  the nuclear spin hyperfine interaction, and  $H_{\text{Z}}$  represents the Zeeman effect of the applied magnetic field. The detailed forms of the operators and their matrix representations in a case (a) basis set are given in Ref. 16, modified slightly in accordance with the recommendation of Ref. 17 to the  $\text{N}^2$  formulation of  $H_{\text{eff}}$ .

The assignment of the observed spectra was, in general, straightforward, the only serious problems being encountered in the assignment of the far IR LMR spectra for the  $^2\Pi_{1/2}$  component. The low tuning rates for the latter transitions often resulted in only part of the germanium isotope structure being recorded in these spectra and it was difficult to identify which particular isotopic species was responsible

TABLE III. Molecular parameters (in MHz) for  $^{74}\text{GeH}$  determined in a fit of the LMR data.

$A + \gamma$	26 757 278.4(67) <sup>a</sup>	$\gamma$	- 14 676(26) <sup>b</sup>
$B$	198 802.16(25)	$10^3 H$	0.3061 <sup>c</sup>
$D$	10.020 2(41)		
$p + 2q$	15 009.1(27)	$p_D + 2q_D$	- 1.512 <sup>c</sup>
$q$	189.80(62)	$10q_D$	- 0.3802 <sup>c</sup>
$h_{1/2}$	38.3(22)	$d$	16.2(19)
$h_{3/2}$	0.0 <sup>c</sup>	$b$	0.0 <sup>c</sup>
$g_L^i$	1.000 77(12)	$10^2 g^r$	- 0.1543(50)
$g_s$	2.0020 <sup>c</sup>	$10(g_i^r - g_r^r)$	0.3953(17)
$10^2 g_i$	0.97(64)	$10^3 g_r^r$	- 0.9552 <sup>c</sup>

<sup>a</sup> The figures in parenthesis denote one standard deviation of the least-squares fit, in units of the last quoted decimal place.

<sup>b</sup> The parameter  $A_D$  was constrained to zero.

<sup>c</sup> Parameter constrained to estimated value in the fit.

TABLE IV. Measurements (in mT) and fit of some resonances in the 166.6  $\mu\text{m}$  LMR spectrum of  $^{73}\text{GeH}$ .

Transition <sup>a</sup>			(obs-calc)/ MHz		(obs-calc)/ MHz
$M_J$	$M_I$	+ ← -		- ← +	
7/2 ← 7/2	- 9/2	b		366.4	0.62
	- 7/2	b		(368.3)	1.03
	- 5/2	303.6	0.05	370.3	0.41
	- 3/2	306.1	0.80	372.5	0.12
	- 1/2	308.5	0.53	374.6	- 1.19
	1/2	310.9	- 0.44	377.5	- 0.51
	3/2	313.9	- 0.10	380.4	- 0.54
	5/2	317.2	0.53	383.8	0.39
	7/2	320.4	0.05	387.2	0.55
	9/2	323.6	- 1.23	b	
5/2 ← 5/2	- 9/2	422.3	- 0.84	516.7	- 0.23
	- 7/2	425.5	- 0.21	518.9	0.40
	- 5/2	427.6	- 0.28	520.8	- 0.16
	- 3/2	430.1	0.15	523.1	- 0.22
	- 1/2	432.6	0.12	525.5	- 0.51
	1/2	435.3	0.10	528.4	- 0.07
	3/2	438.5	0.80	531.2	- 0.36
	5/2	441.5	0.51	534.5	0.07
	7/2	444.6	- 0.07	538.0	0.45
	9/2	448.0	- 0.46	541.7	0.78
Parameters determined in the fit (in MHz):					
$B$	198 841.521(10) <sup>c</sup>	$q$		189.55(19)	
$h_{3/2}$	- 77.69(34)	$eq_0Q$		158.9(76)	

<sup>a</sup>The rotational transition involved is  $^2\Pi_{3/2}$ ,  $J = 9/2 \leftarrow 7/2$ .

<sup>b</sup>Line not measured, overlapped by  $^{74}\text{GeH}$  transition.

<sup>c</sup>The number in parenthesis is one standard deviation of the least-squares fit, in units of the last quoted decimal place.

for the observed resonances. Furthermore, it was hard to anticipate the tuning rates for the different Zeeman components of these transitions since, unlike those for the  $^2\Pi_{3/2}$  component, they are not dominated by the electron spin and orbital  $g$  factors. Careful measurements of the tuning directions of the lines were made by laser frequency "pulling" experiments. These together with the observed relative intensities made it possible to reach a set of unambiguous assignments which satisfied all the experimental observations. The assignments are given in Tables II and IV.

The parameters of the effective Hamiltonian (1) were fitted to the measurements for the dominant isotopic species,  $^{74}\text{GeH}$ , using the computer program described in earlier work.<sup>16,18</sup> The basis set was truncated without loss in accuracy at  $\Delta J = \pm 1$  and the data were weighted as the inverse square of the estimated experimental uncertainties (about 1 MHz for the far IR data and 20 MHz for the 10  $\mu\text{m}$  data). The parameter values determined in the fit are given in Table III. The quality of the fit was very satisfactory with a relative

TABLE V. Proton hyperfine parameters in MHz for GeH and related molecules in their  $X^2\Pi$  states.

	$h_{1/2}$	$b$	$h_{3/2}$	$d$	Reference
CH	64.06	- 76.73	44.50	43.517	25
SiH	34.3	(- 48.3)	4.68	17.9	10
GeH	38.3	...	...	16.2	Present work
SeH	...	...	4.75	...	27

$$h_{1/2} = a - \frac{1}{2}(b + c), \quad h_{3/2} = a + \frac{1}{2}(b + c).$$

standard deviation of 1.19; the residuals for  $^{74}\text{GeH}$  calculated with the parameters in Table III are given in Table II. As can be seen from Table III, it has proved possible to determine all the major parameters of the effective Hamiltonian with the present data set, a notable achievement for the LMR experiment. Some of the smaller parameters had to be constrained to theoretically estimated values which are also given in Table III. The relationships with which these estimates were made are reasonably well established:

$$H_0 \simeq H_e = \frac{3}{2}D_e [12(B_e/\omega_e)^2 - \alpha_e/\omega_e], \quad (2)$$

$$p_D = - 2pD/B, \quad (3)$$

$$q_D = - 4qD/B, \quad (4)$$

and

$$g_r^e = - q/B. \quad (5)$$

Since the proton hyperfine splitting was not resolved for the transitions in the  $^2\Pi_{3/2}$  component, we have set the appropriate parameters ( $h_{3/2}$  and  $b$ ) to zero. The two hyperfine constants determined,  $h_{1/2}$  and  $d$ , describe the splittings of levels in the  $^2\Pi_{1/2}$  component. Our hyperfine parameters are related to those of Frosch and Foley<sup>19</sup> by

$$h_{1/2} = a - \frac{1}{2}(b + c), \quad (6)$$

$$h_{3/2} = a + \frac{1}{2}(b + c). \quad (7)$$

The only other parameter constrained in the fit was the electron spin  $g$  factor  $g_S$ . Since the measurements on the  $^2\Pi_{3/2}$

levels depend on  $(g_L + \frac{1}{2}g_S)$  while those for the  ${}^2\Pi_{1/2}$  levels depend on  $(g_L - \frac{1}{2}g_S)$ , it was a little disappointing that it was not possible to determine separate values for both  $g$  factors. In practice, the separation is confused by the involvement of several smaller contributions to the magnetic moment. The value adopted in Table III was chosen from two considerations. First, it is close to the free electron spin  $g$  value with a small relativistic mass correction.<sup>20</sup> Second, it is a value which leads to reasonably good predictions of the LMR spectra of the other isotopes of GeH. Although the quality of the fit of the  ${}^{74}\text{GeH}$  data can be improved slightly by adopting a larger value for  $g_S$  (about 2.003), such a value leads to much poorer predictions of the spectra of the other isotopes. Some independent information on the zero field frequencies of GeH in the  ${}^2\Pi_{1/2}$  component would probably enable a reliable value for  $g_S$  to be determined.

The 166.6  $\mu\text{m}$  LMR spectrum was strong enough that the lines of  ${}^{73}\text{GeH}$  could be seen in natural abundance, even though each Zeeman transition is split into the ten hyperfine components expected for a nucleus with  $I = 9/2$ . Measurements of some of these lines are given in Table IV. These data were fitted to determine the two nuclear hyperfine parameters for  ${}^{73}\text{GeH}$ ,  $h_{3/2}$ , and  $eq_0Q$ , which govern the splittings of levels in the  ${}^2\Pi_{3/2}$  components. The parameter values determined in the fit are given at the bottom of Table IV. All other parameters were constrained at values obtained by multiplication of those for  ${}^{74}\text{GeH}$  by the appropriate scaling factors.<sup>21</sup>

Finally, we have exploited the observation of electric dipole transitions in the mid-IR spectrum to estimate the magnitude of the electric dipole moment of GeH in its  $X^2\Pi$  state. The relative intensities of electric and magnetic dipole transitions are given by the square of  $\langle i|\boldsymbol{\mu}\cdot\mathbf{E}_\omega|j\rangle/\langle i'|\mathbf{m}\cdot\mathbf{B}_\omega|j'\rangle$  where  $\boldsymbol{\mu}$  and  $\mathbf{m}$  are the electric and magnetic dipole moment operators,  $\mathbf{E}_\omega$  is flux density.<sup>22,23</sup> For an electromagnetic wave in free space,  $E_\omega/B_\omega = 10^{-2}$  c in SI units. In both parallel and perpendicular polarizations of the  $Q(3/2)$  spectrum of GeH at  $880.4\text{ cm}^{-1}$ , there are electric and magnetic dipole transitions of comparable intensity and similar linewidth which lie close to each other in the spectrum (see Table II). We have recorded these regions of the spectra carefully with low modulation amplitude, using a sample enriched in  ${}^{74}\text{GeH}$  to reduce distortion caused by overlap with other isotopic species. From these recordings, we estimate the ratios of the intensities of the electric and magnetic dipole transitions in each polarization. The peak-to-peak height multiplied by the square of the peak-to-peak linewidth was taken as the estimate of the integrated relative intensity. The results from each polarization are pleasingly consistent and lead to the result

$$\mu = 1.24 \pm 0.10 \text{ D.}$$

It should be emphasized that this result is obtained on the assumption that neither electric nor magnetic dipole transition is power saturated. We are fairly sure that this is the case although we cannot be absolutely certain. We know of only one example<sup>24</sup> of power saturation of a magnetic dipole transition in the mid-IR and there was no evidence of Lamb dips on the electric dipole transitions.

## IV. DISCUSSION AND CONCLUSIONS

The paper has been concerned with the characterization of the GeH radical in its ground  ${}^2\Pi$  state. The study is most impressive in its completeness, particularly when it is appreciated that all the data have been collected by laser magnetic resonance techniques. The wide ranging nature of the observations owes much to the sensitivity of the far IR LMR experiment.

### A. Comparison with previous work

The results presented in Tables II, III, and IV show that the effective Hamiltonian in Eq. (1) is sufficiently flexible to fit the experimental data to within the estimated errors. Molecules such as GeH which contain a heavy atom can be expected to provide a stringent test of the second order perturbation theory treatment on which the derivation of the Hamiltonian is based because the large spin-orbit coupling effects and higher order mixing can lead to additional terms in the Hamiltonian.<sup>12</sup> The parameter values determined from our analysis are consistent with those determined earlier from the optical ( $A^2\Delta-X^2\Pi$ ) spectrum<sup>4</sup>:

$$\begin{aligned} B &= 198.77(30) \text{ GHz}, & D &= 9.764(6) \text{ MHz}, \\ A &= 26\,757.1(6) \text{ GHz}, & \tilde{\gamma} &= -14.4(1) \text{ GHz}, \\ p &= 14.87(3) \text{ GHz}, & q &= 215(16) \text{ MHz}, \end{aligned}$$

but, as can be seen in Table III, have much greater precision. The values can also be compared (but with more difficulty) with those quoted by Veseth.<sup>5</sup> His definition for the lambda-doubling parameter  $p$ , e.g., is approximately half that adopted here which makes his value of  $0.248\text{ cm}^{-1}$  or  $7.435\text{ GHz}$  understandable.

### B. Lambda-doubling parameters

The lambda-doubling parameters  $p$  and  $q$  contain information on the electronic wave function for GeH in its  $X^2\Pi$  state. More specifically, they are a measure of the contamination of the ground state by excited  ${}^2\Sigma^+$  and  ${}^2\Sigma^-$  states. A simple model for this mixing has been presented recently for  $\text{CH}$ ,<sup>25</sup> in which the molecular orbitals are represented by atomic orbitals confined to the C atom and only states arising from the first excited configuration are involved. A similar calculation can be performed for GeH. The second order contributions to  $p$  and  $q$  for such a model are

$$p^{(2)} = 2[-\zeta B/(E_\Pi - E_{\Sigma^+}) - B/(E_\Pi - E_{\Sigma^-})] \quad (8)$$

and

$$q^{(2)} = 2[B^2/(E_\Pi - E_{\Sigma^+}) - 3B^2/(E_\Pi - E_{\Sigma^-})], \quad (9)$$

where  $\zeta$  is the atomic spin-orbital coupling parameter,  $B$  is the rotational constant, and  $E_\Pi$ ,  $E_{\Sigma^+}$ , and  $E_{\Sigma^-}$  are the energies of the  ${}^2\Pi$ ,  ${}^2\Sigma^+$ , and  ${}^2\Sigma^-$  electronic states, respectively. The large spin-orbit interactions in GeH suggest that higher order contributions to these parameters may not be negligible marking a tendency towards Hund's case (c) coupling.<sup>5,12</sup> The leading third order contribution to  $p$ , which involves admixture of the  $a^4\Sigma^-$  state, may be estimated in the same way as the second order contributions to be

$$p^{(3)} = \frac{2}{3}\zeta B^2/(E_\Pi - E_{\Sigma^-})^2, \quad (10)$$



where  $E_{\Sigma^-}$  is the energy of the  $^4\Sigma^-$  state. Unfortunately, rather few excited electronic states have been characterized for GeH. Only one  $^2\Sigma$  state has been identified and that not even with absolute certainty.<sup>3</sup> It has yet to be established whether it is the  $^2\Sigma^+$  or  $^2\Sigma^-$  state arising from the first excited electronic configuration. If we assume that the  $^2\Sigma^+$  and  $^2\Sigma^-$  states lie very close in energy at this value of 42 703  $\text{cm}^{-1}$  above the ground state, we can at least make a rough estimate of the values for  $p$  and  $q$ , namely,

$$p^{(2)} = 17.3 \text{ GHz}, \quad p^{(3)} = 420 \text{ MHz}, \quad \text{and} \quad q^{(2)} = 128 \text{ MHz}.$$

These are in reasonable agreement with the experimental values ( $p = 14.6 \text{ GHz}$ ,  $q = 189.8 \text{ MHz}$ ), particularly when the grossness of the assumptions made is taken into account.

In a similar study of SeH, Brown *et al.*<sup>12</sup> found that it was necessary to include the effects of centrifugal distortion of lambda doubling in order to reproduce the experimental results. The parameters involved,  $p_D$  and  $q_D$ , may be estimated if the electronic wave function is assumed to be independent of the internuclear distance.<sup>26</sup> The relations are given in Eqs. (3) and (4) and the values deduced in Table III. These values are about an order of magnitude smaller than the corresponding ones for SeH and had an insignificant effect on the quality of fit.

### C. Nuclear hyperfine parameters

Two of the four proton hyperfine parameters for  $^{74}\text{GeH}$  fit have been determined in our fit (see Table III). It is worth mentioning that the signs of these parameters have been determined unambiguously from the relative intensities of lines in the  $^2\Pi_{3/2}$  transitions. For example, a small but real difference in the intensities of the lines in the low field doublet can be seen in Fig. 2. The effect was more marked in other transitions. The values determined for  $^{74}\text{GeH}$  can be compared with those for related molecules in Table V. The values for SiH, GeH, and SeH are rather similar, all of them significantly smaller than the corresponding parameters for CH. This behavior broadly follows the trend in values for  $r^{-3}$  where  $r$  is the bond length. (The  $r_e$  values for CH, SiH, and GeH are 0.1120, 0.1520, and 0.1588 nm, respectively).<sup>28</sup> Unfortunately, we have no indication of the size of the Fermi contact interaction in GeH from the present data set. More precise measurements, by techniques such as microwave optical double resonance, are required.

The  $^{73}\text{Ge}$  hyperfine splittings in GeH have been fitted as described in Table IV. In this case, the data set is rather limited and the sign of the parameter  $h_{3/2}$  is assumed from the negative value for the nuclear magnetic moment  $g_N = -0.1984$ .<sup>29</sup> Nevertheless, this is the first experimental determination of a magnetic hyperfine interaction involving  $^{73}\text{Ge}$ . Clearly more measurements are needed on this isotopic modification if the complete set of hyperfine parameters is to be determined and the full worth of information on the electronic wave function extracted.

### D. Zeeman parameters

The  $g$  factors determined from the magnetic resonance data also contain information on the electronic wave function. Of the values listed in Table IV, two can be compared

with values estimated on the basis of simple formulas, namely,

$$g_l = -\gamma/2B = 0.0369 \quad (11)$$

and

$$g'_l = p/2B = 0.0368. \quad (12)$$

The experimental values from Table IV are 0.01 and 0.0386, respectively. It is clear that Eq. (12) provides a much more reliable estimate than Eq. (11). Similar results were obtained for CH<sup>9,25</sup> and SiH.<sup>10</sup> The value for  $g_l$  in Eq. (11) is less reliable than it might be because of the use of the value for the effective spin-rotation parameter  $\tilde{\gamma}$  (which contains a contribution from  $A_D$ ) rather than the value for  $\gamma$  itself. The orbital  $g$  factor  $g'_l$  contains information about the mixing of excited electronic states by spin-orbit coupling.<sup>16,12</sup> Unfortunately, the value obtained in the fit depends critically on the value adopted for  $g_s$ . For a molecule like GeH, the latter parameter is hard to estimate since it probably contains significant third order contributions,<sup>30</sup> particularly from the  $a^4\Sigma^-$  state. In view of these uncertainties, it is not meaningful to pursue an interpretation of the orbital  $g$  factor at this juncture.

### E. Electric dipole moment

We have reported a measurement of the electric dipole moment of GeH in its ground  $^2\Pi$  state from a comparison of the intensities of electric and magnetic dipole transitions. It was surprising to discover that the variation of the dipole moment down the series CH, SiH, and GeH was rather irregular; the values are 1.46,<sup>31</sup> 0.124,<sup>32</sup> and 1.24 D, respectively. The value for GeH is consistent with the strong LMR spectra recorded in our work and the observation of Lamb dips on the strongest lines. Equally, the very small value calculated for SiH is consistent with the rather weak LMR spectra recorded for that molecule and our inability to record Lamb dips in that case.<sup>10</sup> There is no doubt that the trend is genuine but an explanation is not easy to discover. It is possible that the polarity of the dipole moment changes down the series (the experimental observations depend only on its magnitude). A theoretical study of GeH is in progress to investigate the observed behavior.<sup>33</sup>

### F. Further work

We have described a broad-ranging study of the ground state of GeH by a combination of far- and midinfrared LMR techniques. Although the major parameters can now be considered to be well determined, uncertainties remain for some of the minor ones such as the hyperfine parameters. Measurements on GeH in the microwave region would remove most of these deficiencies and be well worth while. The spectra described in this work also show a wealth of isotopic structure. We have exploited this structure qualitatively in our analysis but there are quantitative implications which we have not followed up. It would be very interesting to fit all the isotopic data in Table II simultaneously. In addition to testing the various isotopic dependences of the parameters, there are strong indications that additional information on GeH in its  $X^2\Pi$  state can be wrested from the data. By the

same token, a parallel study of GeD would be interesting. There are suggestions in the optical work that the spin-orbit interaction shows an anomalously large isotopic dependence.<sup>4,5</sup> Furthermore, the fundamental vibration-rotation band of GeH lies at about  $1830\text{ cm}^{-1}$ ,<sup>4</sup> a region well suited to study by LMR using a carbon monoxide laser.

#### ACKNOWLEDGMENTS

We are grateful to Liz Comben for help with some of the computation. We also acknowledge the assistance of M. Wong in early searches for germanium and hydrogen containing radicals at the National Research Council of Canada. Research at Brookhaven Laboratory was carried out under Contract No. DE-AC02-76CH00016 with the U. S. Department of Energy and supported by its Office of Basic Energy Sciences. T. J. S. thanks the National Research Council of Canada for support during the time that part of this work was carried out.

- <sup>1</sup>B. Kleman and E. Werhagen, *Ark. Fys.* **6**, 359 (1953).
- <sup>2</sup>B. Kleman and E. Werhagen, *Ark. Fys.* **6**, 399 (1953).
- <sup>3</sup>R. F. Barrow, G. Drummond, and W. R. S. Garton, *Proc. Phys. Soc. London, Sect. A* **66**, 191 (1953).
- <sup>4</sup>L. Klynning and B. Lindgren, *Ark. Fys.* **32**, 575 (1966).
- <sup>5</sup>L. Veseth, *J. Mol. Spectrosc.* **48**, 283 (1973).
- <sup>6</sup>K. M. Evenson, *Faraday Discuss. Chem. Soc.* **71**, 7 (1981).
- <sup>7</sup>A. R. W. McKellar, *Faraday Discuss. Chem. Soc.* **71**, 63 (1981).
- <sup>8</sup>J. T. Hougen, J. A. Mucha, D. A. Jennings, and K. M. Evenson, *J. Mol. Spectrosc.* **72**, 463 (1973).
- <sup>9</sup>J. M. Brown and K. M. Evenson, *J. Mol. Spectrosc.* **98**, 392 (1983).
- <sup>10</sup>J. M. Brown, R. F. Curl, and K. M. Evenson, *J. Chem. Phys.* **81**, 2884 (1984).
- <sup>11</sup>G. Herzberg, *Molecular Spectra and Structure I. Diatomic Molecules* (Van Nostrand, New York, 1950).
- <sup>12</sup>J. M. Brown, A. Carrington, and T. J. Sears, *Mol. Phys.* **37**, 1837 (1979).
- <sup>13</sup>A. R. W. McKellar, *J. Mol. Spectrosc.* **86**, 43 (1981).
- <sup>14</sup>R. M. Dale, J. W. C. Johns, A. R. W. McKellar, and M. Rigglin, *J. Mol. Spectrosc.* **67**, 440 (1977).
- <sup>15</sup>R. S. Lowe and A. R. W. McKellar, *J. Mol. Spectrosc.* **79**, 424 (1978).
- <sup>16</sup>J. M. Brown, M. Kaise, C. M. L. Kerr, and D. J. Milton, *Mol. Phys.* **36**, 553 (1978).
- <sup>17</sup>J. M. Brown, E. A. Colbourn, J. K. G. Watson, and F. D. Wayne, *J. Mol. Spectrosc.* **74**, 294 (1979).
- <sup>18</sup>J. M. Brown, C. M. L. Kerr, F. D. Wayne, K. M. Evenson, and H. E. Radford, *J. Mol. Spectrosc.* **86**, 544 (1981).
- <sup>19</sup>R. A. Frosch and H. M. Foley, *Phys. Rev.* **88**, 1337 (1952).
- <sup>20</sup>A. Abragam and J. H. Van Vleck, *Phys. Rev.* **92**, 1448 (1953).
- <sup>21</sup>J. M. Brown and A. D. Fackerell, *Phys. Scr.* **25**, 351 (1982).
- <sup>22</sup>H. E. Radford, *Phys. Rev.* **112**, 114 (1961).
- <sup>23</sup>A. Carrington, D. H. Levy, and T. A. Miller, *Adv. Chem. Phys.* **18**, 149 (1970).
- <sup>24</sup>V. R. Braun, L. N. Krasnoperov, and V. N. Panfilov, *Opt. Spectrosc.* **52**, 428 (1982).
- <sup>25</sup>C. R. Brazier and J. M. Brown, *Can. J. Phys.* **62**, 1563 (1984).
- <sup>26</sup>R. S. Mulliken and A. Christy, *Phys. Rev.* **38**, 87 (1931).
- <sup>27</sup>H. E. Radford, *J. Chem. Phys.* **40**, 2732 (1964).
- <sup>28</sup>K.-P. Huber and G. Herzberg, *Constants of Diatomic Molecules* (Van Nostrand-Reinhold, New York, 1979).
- <sup>29</sup>C. H. Townes and A. L. Schawlow, *Microwave Spectroscopy* (McGraw-Hill, New York, 1955), p. 645.
- <sup>30</sup>J. M. Brown, K. Dumper, and C. R. Parent, *Mol. Phys.* **36**, 1149 (1978).
- <sup>31</sup>D. H. Phelps and F. W. Dalby, *Phys. Rev. Lett.* **16**, 3 (1966).
- <sup>32</sup>M. Lewerenz, P. J. Bruna, S. D. Peyerimhoff, and R. J. Buenker, *Mol. Phys.* **49**, 1 (1983).
- <sup>33</sup>H. J. Werner and A. D. Buckingham (private communication).